

Effects of pH and Low Density Lipoprotein (LDL) on PCSK9-dependent LDL Receptor Regulation^{*[S]}

Received for publication, February 23, 2007, and in revised form, May 10, 2007 Published, JBC Papers in Press, May 10, 2007, DOI 10.1074/jbc.M701634200

Timothy S. Fisher[‡], Paola Lo Surdo[§], Shilpa Pandit[‡], Marco Mattu[§], Joseph C. Santoro[‡], Doug Wisniewski[¶], Richard T. Cummings[‡], Alessandra Calzetta[§], Rose M. Cubbon[‡], Paul A. Fischer[¶], Anil Tarachandani[¶], Raffaele De Francesco[§], Samuel D. Wright[‡], Carl P. Sparrow[‡], Andrea Carfi^{§1}, and Ayesha Sitlani^{‡2}

From the Departments of [‡]Cardiovascular Diseases, [¶]Infectious Diseases, and [¶]Target Validation, Merck Research Laboratories, Rahway, New Jersey 07065 and the [§]Istituto di Ricerche di Biologia Molecolare "P. Angeletti", 00040 Pomezia, Rome, Italy

Mutations within PCSK9 (proprotein convertase subtilisin/kexin type 9) are associated with dominant forms of familial hyper- and hypocholesterolemia. Although PCSK9 controls low density lipoprotein (LDL) receptor (LDLR) levels post-transcriptionally, several questions concerning its mode of action remain unanswered. We show that purified PCSK9 protein added to the medium of human endothelial kidney 293, HepG2, and Chinese hamster ovary cell lines decreases cellular LDL uptake in a dose-dependent manner. Using this cell-based assay of PCSK9 activity, we found that the relative potencies of several PCSK9 missense mutants (S127R and D374Y, associated with hypercholesterolemia, and R46L, associated with hypocholesterolemia) correlate with LDL cholesterol levels in humans carrying such mutations. Notably, we found that *in vitro* wild-type PCSK9 binds LDLR with an ~150-fold higher affinity at an acidic endosomal pH ($K_D = 4.19$ nM) compared with a neutral pH ($K_D = 628$ nM). We also demonstrate that wild-type PCSK9 and mutants S127R and R46L are internalized by cells to similar levels, whereas D374Y is more efficiently internalized, consistent with their affinities for LDLR at neutral pH. Finally, we show that LDL diminishes PCSK9 binding to LDLR *in vitro* and partially inhibits the effects of secreted PCSK9 on LDLR degradation in cell culture. Together, the results of our biochemical and cell-based experiments suggest a model in which secreted PCSK9 binds to LDLR and directs the trafficking of LDLR to the lysosomes for degradation.

PCSK9 (proprotein convertase subtilisin/kexin type 9) encodes the ninth member of the mammalian proprotein convertase family of serine endoproteases. PCSK9 is translated as a 692-amino acid proprotein that includes several domains found in other proprotein convertases, including an N-terminal signal sequence, a prodomain, a catalytic domain, and a cysteine-rich C-terminal domain (1–3). The PCSK9 catalytic domain shares

high sequence similarity with the proteinase K family of subtilases and contains a catalytic triad (Asp¹⁸⁶, His²²⁶, and Ser³⁸⁶) responsible for autoprocessing (1, 4). PCSK9 processing occurs in the secretory pathway, presumably in the endoplasmic reticulum, and results in proteolytic cleavage occurring after Gln¹⁵² (FAQ ↓ SIP). This cleavage generates a stable PCSK9 heterodimer composed of a 14-kDa prodomain fragment and a mature 57-kDa fragment containing the catalytic and C-terminal domains (4, 5). Following processing, the PCSK9 heterodimer exits the ER and is eventually secreted (1). The prodomain of PCSK9 remains strongly bound to the mature protein after secretion, presumably inhibiting the catalytic activity of PCSK9 (1, 5, 6). To date, there is no conclusive evidence that the processed secreted form of PCSK9 can cleave any substrates in a catalytic serine-dependent manner.

The first evidence that PCSK9 plays a significant role in regulating plasma low density lipoprotein (LDL)³ cholesterol (LDL-C) levels was the identification of several missense mutations in PCSK9 resulting in a form of autosomal dominant hypercholesterolemia (7–9). Mutations within the prodomain (S127R) or catalytic domain (F216L and D374Y) are associated with high levels of circulating LDL-C. In addition to PCSK9 mutations that result in hypercholesterolemia, two large genetic studies identified two nonsense mutations (Y142X and C679X) and several missense mutations (R46L, L253F, and A443T) in PCSK9 that are associated with hypocholesterolemia (10–12). Notably, humans that are heterozygous for either the Y142X or C679X truncation mutation have a 30–40% reduction in plasma LDL-C and an 88% reduction in the risk of coronary heart disease (13). In comparison, humans heterozygous for the R46L missense mutation have a 15% reduction in LDL-C and a 47% reduction in cardiovascular disease (13). Based on their relative effects on plasma LDL-C concentrations in humans and the fact that certain PCSK9 mutations (S127R, F216L, and D374Y) cause dominant hypercholesterolemia, PCSK9 mutations have been classified as either loss-of-function (Y142X, C679X, and R46L) or gain-of-function (S127R, F216L, and D374Y) mutations.

* The costs of publication of this article were defrayed in part by the payment of page charges. This article must therefore be hereby marked "advertisement" in accordance with 18 U.S.C. Section 1734 solely to indicate this fact.

[S] The on-line version of this article (available at <http://www.jbc.org>) contains supplemental Figs. 1–III.

¹ To whom correspondence may be addressed. Tel.: 39-06-9109-3550; Fax: 39-06-9109-3225; E-mail: andrea_carfi@merck.com.

² To whom correspondence may be addressed: Dept. of Cardiovascular Diseases, Merck Research Laboratories, PO Box 2000, Mail Code RY80Y-300, Rahway, NJ 07065. Tel.: 732-594-0788; Fax: 732-594-1169; E-mail: ayesha_sitlani@merck.com.

³ The abbreviations used are: LDL, low density lipoprotein; LDL-C, low density lipoprotein cholesterol; LDLR, low density lipoprotein receptor; HEK, human embryonic kidney; DMEM, Dulbecco's modified Eagle's medium; FBS, fetal bovine serum; VLDL, very low density lipoprotein; Dil, 3,3'-dioctadecylindocarbocyanine; BSA, bovine serum albumin; TR-FRET, time-resolved fluorescence resonance energy transfer; CHO, Chinese hamster ovary.

Several lines of evidence demonstrate that PCSK9 lowers the amount of hepatic LDL receptor (LDLR) protein and thus compromises the liver's ability to remove LDL-C from the circulation. Adenovirus-mediated overexpression of PCSK9 in the livers of mice results in the accumulation of circulating LDL-C because of a dramatic loss of hepatic LDLR protein, with no effect on LDLR mRNA levels (5, 14–16). The effect of PCSK9 overexpression on raising circulating LDL-C levels in mice is completely dependent on the expression of LDLR, again indicating that the regulation of LDL-C by PCSK9 is mediated through down-regulation of LDLR protein. In agreement with these findings, mice lacking PCSK9 or in which PCSK9 mRNA has been lowered by antisense oligonucleotide inhibitors have higher levels of hepatic LDLR protein and a greater ability to clear circulating LDL-C (17, 18). In addition, lowering PCSK9 levels in cultured human hepatocytes by small interfering RNA also results in higher LDLR protein levels and an increased ability to take up LDL-C (5, 16). Together, these data indicate that PCSK9 action leads to increased LDL-C by lowering LDLR protein levels.

Although PCSK9 post-transcriptionally reduces the amount of LDLR, the mechanism and site of PCSK9 action remain unresolved. Recent observations indicate that PCSK9 can regulate LDLR protein levels both during and after secretion (6, 19). Moreover, a recent study has demonstrated using non-quantitative gel-based methods that PCSK9 binds specifically to LDLR and that the gain-of-function mutant D374Y shows increased binding *in vitro* (6). In this study, we compare the effects of processed secreted forms of wild-type PCSK9, gain-of-function mutants D374Y and S127R, and loss-of-function mutant R46L on cellular LDL uptake as a measure of LDLR function. Using surface plasmon resonance (Biacore) experiments, we also obtained kinetic and thermodynamic binding constants for the interaction between LDLR and wild-type and S127R, D374Y, and R46L mutant PCSK9. Our functional and biochemical data collectively suggest a mechanism whereby processed secreted PCSK9 binds to LDLR and likely prevents LDLR cell-surface recycling by directing the receptor to the lysosomes for degradation.

EXPERIMENTAL PROCEDURES

Construction of Wild-type and Mutant PCSK9 Expression Vectors

The *PCSK9* gene was amplified from human fetal liver QUICK-Clone cDNA (BD Biosciences). The following primers were used for the pre-amplification of the *PCSK9* cDNA: 5'-GCAACCTCTCCCCTGGCCCTCATG-3' (forward) and 5'-GCTTCCTGGCACCTCCACCTGGGG-3' (reverse). This *PCSK9* gene product was used as a template for TOPO TA primers to generate the final PCSK9 sequence. The primers for TOPO TA cloning were 5'-CCACCATGGGCACCGTCAGC-TCCAGG-3' (forward) and 5'-CTGGAGCTCCTGGGAGGC-CTGCGCCAG-3' (reverse). The final PCSK9 insert was ligated into a TOPO TA vector using a pcDNA3.1/V5-His-TOPO-TA expression kit (Invitrogen), followed by transformation into chemically competent TOP10 *Escherichia coli* cells. Clones

were selected and checked for the correct insert by gel electrophoresis. Based on sequence analysis of this clone, it is important to note that this sequence has the more common form of the two natural mutations I474V and E670G and matches GenBank™ accession number AX207686. The plasmid containing wild-type PCSK9 with C-terminal V5 and His tags is referred to as pcDNA3.1-F1-WT.

To generate plasmids expressing mutant forms of human PCSK9, site-directed mutagenesis was performed using the QuikChange II XL site-directed mutagenesis kit (Stratagene). The following primers were used to generate mutations: for plasmid pcDNA3.1-F1-S386A, 5'-CACAGAGTGGGACAG-CACAGGCTGCTGCCAC-3' (forward) and 5'-GTGGG-CAGCAGCCTGTGCTGTCCACTCTGTG-3' (reverse); for plasmid pcDNA3.1-F1-S127R, 5'-CTGGTGAAGATGAG-GGGCGACCTGCTGG-3' (forward) and 5'-CCAGCAGG-TCGCCCCTCATCTCACCAG-3' (reverse); for plasmid pcDNA3.1-F1-D374Y, 5'-CATTGGTGCCTCCAGCTACTG-CAGCACCTGC-3' (forward) and 5'-GCAGGTGCTGCAGT-AGCTGGAGGCACCAATG-3' (reverse); and for plasmid pcDNA3.1-R46L, 5'-CTGGTGTAGCCTTGCTGTCCG-AGGAGGACGGCC-3' (forward) and 5'-GGCCGTCTC-CTCGGACAGCAAGGCTAGCACCAG-3' (reverse). All PCSK9 constructs described were present in a pcDNA3.1 backbone with G418 selection and C-terminal V5 and His tags (Invitrogen).

Stable Transfection of Human Embryonic Kidney (HEK) 293 Cells

HEK293 cells were plated at a density of 1.8×10^6 cells/6-well container in $1 \times$ Dulbecco's modified Eagle's medium (DMEM; Mediatech, Inc.) containing 100 units of penicillin and 100 $\mu\text{g}/\text{ml}$ streptomycin sulfate and supplemented with 10% fetal bovine serum (FBS). The following day, cells were transfected with 6 μg of wild-type or mutant plasmid DNA per container using FuGENE 6 transfection reagent (Roche Applied Science) according to the manufacturer's instructions. A reagent/plasmid DNA ratio of 6:1 was used for transfections. To generate a control stable cell line, 6 μg of pcDNA3.1 was used to transfect HEK293 cells. After 2 days, the medium was changed to $1 \times$ DMEM containing 1 mg/ml G418 and supplemented with 10% FBS, and cells were maintained in this medium.

Western Blot Analysis

PCSK9 Western Blot Analysis—Cells carrying vector alone (pcDNA3.1) or vector plus PCSK9 (pcDNA3.1-F1-WT, pcDNA3.1-F1-R46L, pcDNA3.1-F1-S127R, and pcDNA3.1-F1-D374Y) were plated in $1 \times$ DMEM containing 1 mg/ml G418 and supplemented with 10% FBS. After 24 h, the medium was switched to DMEM lacking serum. After an additional 6 h, the medium was removed, and the cells were lysed in radioimmune precipitation assay buffer (Teknova) plus Complete protease inhibitor mixture (Roche Applied Science). Protein concentration was assayed using a BCA protein assay kit (Pierce). 10 μg of proteins from lysate or 15 μl of medium was loaded onto 10–20% Tris/glycine gels (Invitrogen). Following transfer, membranes were successively incubated with anti-V5 primary antibody (1:5000; Invitrogen) and alkaline phosphatase-conju-

Secreted PCSK9 Regulates LDL Uptake

gated anti-mouse IgG (H + L) (1:3000; Promega). Bands were subsequently detected using a one-step nitro blue tetrazolium/5-bromo-4-chloro-3-indolyl phosphate kit (Pierce) according to the manufacturer's instructions.

LDLR Western Blotting—HEK293 cells carrying vector alone (pcDNA3.1) were plated in a 24-well plate in 1× DMEM containing 1 mg/ml G418 and supplemented with 10% FBS. After 24 h, the medium was switched to DMEM lacking serum. Cells were further incubated for 24 h without serum, and each well containing $\sim 1.2 \times 10^5$ cells was lysed in 160 μ l of radioimmune precipitation assay buffer. Lysate (40 μ l) was loaded onto 4–12% NuPAGE gel (Invitrogen). Following transfer, membranes were incubated with rabbit anti-human LDLR antibody (Research Diagnostics Inc.) and horseradish peroxidase-conjugated anti-rabbit IgG (H + L) (Cell Signaling Technology). Bands were subsequently detected using an ECL kit (Amersham Biosciences) according to the manufacturer's instructions.

PCSK9 Purification

The medium generated from one cell factory was stored at 4 °C. TALON immobilized metal affinity chromatography resin (10 ml; Clontech) was added and rocked at room temperature for 1 h on an Adams Nutator. Resin was collected by gravity filtration and bulk-washed according to reagent instructions. Less than 10 mg of eluted protein (concentration determined by absorbance at 280 nm using a NanoDrop ND-1000 spectrophotometer) was loaded onto a Superdex 200 10/300 GL size exclusion column (GE Healthcare) run in buffer A (25 mM HEPES, 30 mM NaCl, 0.1 mM CaCl₂, and 5% glycerol, pH 7.9). Peak fractions were loaded onto a 6-ml RESOURCE Q column (GE Healthcare). A 6.0 ml/min linear gradient of 0–50% elution buffer A plus 1.0 M NaCl in a volume of 120 ml was used. Peak fractions were concentrated using a Centricon Centriplus-5 concentrator (Millipore) to concentrations of >1 mg/ml and stored at –20 °C. For Biacore studies, proteins were purified by immobilized metal affinity chromatography and then loaded, after extensive dialysis, onto a RESOURCE Q column. Peak fractions were pooled and loaded onto a Superdex 200 20/60 size exclusion column (GE Healthcare) run in 25 mM HEPES, 150 mM NaCl, 0.1 mM CaCl₂, and 10% glycerol, pH 7.9. Concentrated proteins (up to 10 mg/ml) were stored at –80 °C.

Isolation of LDL

Blood for LDL isolation was obtained from healthy human volunteers. Blood (200 ml) was collected in EDTA tubes and spun at 15,000 rpm for 15 min at 4 °C. Plasma density was adjusted to 1.02 g/ml with sodium bromide, and the tubes were centrifuged at 45,000 rpm in a Ti-70 ultracentrifuge rotor for 20 h. The very LDL (VLDL) layer was removed, and the bottom layer was adjusted to a density of 1.063 g/ml with sodium bromide. The tubes were again centrifuged at 45,000 rpm in a Ti-70 rotor for 72 h. The LDL layer was removed and dialyzed against phosphate-buffered saline, pH 7.4, and 1 mM EDTA. The final protein concentration was determined using the BCA protein assay kit.

Labeling of LDL, PCSK9, LDLR, and Anti-V5 Antibody

LDL was labeled with a fluorescent 3,3'-dioctadecylindocarbocyanine (DiI) particle (Molecular Probes). A stock solution containing 3 mg of DiI dissolved in 1 ml of Me₂SO was prepared. This stock solution of DiI was added to LDL at a final concentration of 135 μ g of DiI to 1 ml of LDL (1 mg/ml). The labeling reaction was incubated at 37 °C for 24 h in the dark, followed by LDL isolation as described above.

PCSK9 protein and anti-V5 antibody were labeled with Alexa Fluor 647. Prior to labeling, proteins (0.5–2 mg/ml) were buffer-exchanged into 100 mM sodium carbonate and 200 mM NaCl, pH 8.6, at 4 °C using D-Tube dialyzers (Calbiochem). Proteins were then reacted with either 5 (PCSK9) or 10 (anti-V5 monoclonal antibody) molar eq of Alexa Fluor 647-labeled *N*-hydroxysuccinimide (Invitrogen) that had been dissolved in Me₂SO at 10 mg/ml. Alexa Fluor 647 was added, and the solution briefly was vortexed and allowed to stand at 4 °C for at least 4 h protected from light. The reaction was quenched by the addition of 1.0 M Tris, pH 8.0, to a final concentration of at least 10 mM for 30 min. Purification from free dye was achieved using a NAP-5 column (GE Healthcare) pre-equilibrated in 50 mM potassium phosphate and 350 mM NaCl, pH 7.0, and eluted with the same buffer. Protein concentration and extent of dye incorporation were determined by measuring the relative absorbance at 280 and 651 nm and the extinction coefficients for the Alexa Fluor 647 dye provided by the manufacturer. Labeled proteins were stabilized by the addition of bovine serum albumin (BSA; Sigma) to a final concentration of 0.05% (w/v).

Soluble LDLR (R&D Systems) was labeled with europium as described below. Lyophilized soluble LDLR (50 μ g, 560 pmol) was solubilized in 100 μ l of 100 mM sodium carbonate and 200 mM NaCl, pH 8.6, and dialyzed against the same buffer at 4 °C using D-Tube dialyzers. The material was combined with 7.1 μ l of a 10 mg/ml solution of Europium (W1024) isothiocyanate (Eu-W1024-ITC) (PerkinElmer Life Sciences) dissolved in water (71 μ g, 10 nmol, 20 eq). Labeling was carried out for \sim 16 h at 4 °C protected from light; quenched by the addition of 1.0 M Tris, pH 8.0, to a final concentration of 100 mM for 15 min; and brought to a total volume of 100 μ l with 50 mM potassium phosphate and 350 mM NaCl, pH 7.0. Purification from free europium was achieved using a two-step process: 1) rapid buffer exchange using a Bio-Spin 30 column (Bio-Rad) pre-equilibrated in 50 mM potassium phosphate and 350 mM NaCl, pH 7.0, immediately followed by the addition of a 5% (w/v) BSA stock to a final concentration of 0.05%; and 2) further purification by a NAP-5 column pre-equilibrated in 50 mM potassium phosphate, 350 mM NaCl, pH 7.0, and 0.05% BSA and elution with the same solution. Because of the low amounts of soluble LDLR, available protein concentration was not determined explicitly. Time-resolved fluorescence resonance energy transfer (TR-FRET) experiments described below are reported using the *maximum* concentration assuming 100% recovery from labeling.

DiI-labeled LDL Uptake Assay

HEK293 cells stably expressing the pcDNA3.1 vector alone were plated in a 96-well poly-D-lysine-coated plate (Corning) at

a density of 30,000 cells/well in $1 \times$ DMEM containing 1 mg/ml G418 and 10% FBS. A similar plating protocol was followed for HepG2 and Chinese hamster ovary (CHO) cells, except that G418 was not added to the medium. After 24 h, the medium was switched to either DMEM lacking serum or containing 10% lipoprotein-deficient serum (Intracel), with either protocol yielding similar potencies for PCSK9. After 18 h, the medium was removed, and the cells were washed with Opti-MEM (Invitrogen). Purified PCSK9 protein was added to the cells in 100 μ l of mixture A (DMEM containing 10% lipoprotein-deficient serum and 10 μ g/ml DiI-labeled LDL). To measure non-specific binding, 100 μ l of mixture A that also contained 400 μ g/ml unlabeled LDL was added to control wells. The plates were incubated at 37 °C for 6.5 h, and the cells were washed quickly with Tris-buffered saline (Bio-Rad) containing 2 mg/ml BSA. The wash step was repeated, but this time the wash buffer was incubated for 2 min with the cells. Finally, the cells were quickly washed twice with Tris-buffered saline (without BSA) and lysed in 100 μ l of radioimmune precipitation assay buffer. The lysate was transferred to a 96-well black plate (Thermo LabSystems), and fluorescence was measured using a Spectra-MAX tunable spectrofluorometer (Molecular Devices) at an excitation wavelength of 520 nm and an emission wavelength of 580 nm. Total cellular protein was measured in each well using the BCA protein assay, and the fluorescence units were normalized to total protein. The amount of specific LDL uptake (specific counts) is the difference between the total counts measured (in the absence of unlabeled LDL) and the counts measured in the presence of an excess of unlabeled LDL (non-specific background fluorescence). The amount of PCSK9 protein required for 50% inhibition of DiI-labeled LDL uptake (EC_{50}) was determined by fitting data to a sigmoidal dose-response curve using nonlinear regression (GraphPad Software Inc.).

PCSK9-LDLR Binding Affinity Measurements

Surface Plasmon Resonance (Biacore)—The interaction between the LDLR ectodomain and wild-type PCSK9 or the D374Y, S127R, and R46L variants was studied by surface plasmon resonance detection using a Biacore 3000 instrument (20, 21). A commercial LDLR ectodomain (residues 22–788; 10 μ g/ml in 10 mM sodium acetate, pH 5.0; R&D Systems) was coupled to a research-grade carboxymethylated dextran sensor chip (CM5, Biacore) using the amine coupling kit supplied by the manufacturer to give surface densities of \sim 150 resonance units. Wild-type and mutant PCSK9 proteins were injected at a concentration range of 0.03–2.0 μ M in a running buffer of 25 mM HEPES, pH 7.4, 150 mM NaCl, and 0.1 mM $CaCl_2$. For studies at acidic pH, experiments were carried out in 25 mM sodium acetate, pH 5.3, 150 mM NaCl, and 0.1 mM $CaCl_2$ with PCSK9 concentrations spanning 0.03–0.5 μ M. Injections were performed at 25 °C with flow rates of 40 μ l/min. Sensor chip surfaces were regenerated with 50 mM HCl for 3 s. The LasR ligand-binding domain was used as a control to exclude non-specific binding of the PCSK9 protein to immobilized LDLR. Competition experiments between wild-type PCSK9 and LDL particles for binding LDLR were performed by incubating samples of LDLR with increasing concentrations of wild-type

PCSK9 (0–2 μ M) before injection over immobilized LDL particles. The primary data were analyzed using BIAevaluation Version 4.1 software. Base lines were adjusted to zero for all curves, and injection start times were aligned. The reference sensorgrams were then subtracted from the experimental sensorgrams to yield curves representing specific binding. All of the kinetic data were fit by assuming a simple 1:1 reaction model for interaction between soluble analyte and immobilized ligand, equivalent to the Langmuir isotherm for adsorption to a surface.

Steady-state analysis was used to obtain thermodynamic dissociation constants (K_D) at pH 7.4. For each single titration, simultaneous fitting of all the dissociation curves was used to obtain k_{off} values. k_{on} values were calculated from K_D and k_{off} values ($K_D = k_{off}/k_{on}$). For the binding data at pH 5.3, k_{on} and k_{off} were obtained by separate fitting of all the association and dissociation curves of each titration, respectively. These kinetic constants were then used to calculate the K_D values.

TR-FRET—PCSK9-LDLR interactions were also studied by TR-FRET (22, 23). This involved preparing fluorescently labeled LDLR, PCSK9, and anti-V5 monoclonal antibody to PCSK9-V5-His as described above. TR-FRET experiments were carried out in 96-well black Microfluor-2 U-bottom plates (Dyex Technologies). Samples were 50- μ l total volume in 10 mM HEPES, pH 7.4, 150 mM NaCl, 0.1 mM $CaCl_2$, and 0.05% (w/v) BSA. The concentrations of reagents are as noted in individual experiments, except for europium-labeled LDLR, for which the stated concentration is the *maximum* assuming 100% recovery after labeling. Regardless of the putative concentration, europium-labeled LDLR was used at 20,000–40,000 total counts at 620 nm. All materials were prepared in-house as described, except for VLDL, which was purchased commercially (Intracel). Samples were read using a BMG LabSystems Rubystar Reader set to read 20 flashes/well with a 50- μ s integration delay and a 200- μ s integration time for a total read time of 1100 ms/well. Data are reported as the ratio of (counts at 665 nm/counts at 620 nm) \times 10,000.

PCSK9 Cellular Uptake

Cells treated with Alexa Fluor 647-labeled PCSK9 were imaged as follows. CHO cells were plated on poly-D-lysine-coated 96-well optical CVG sterile black plates (Nunc) at a density of 20,000 cells/well. Cells were plated in F-12K medium (nutrient mixture, Kaighn's modification (1 \times)) (Invitrogen) containing 100 units of penicillin and 100 μ g/ml streptomycin sulfate and supplemented with 10% FBS. Plates were incubated overnight at 37 °C and 5% CO_2 . The following morning, the medium was removed and replaced with 100 μ l of F-12K medium containing 100 units of penicillin and 100 μ g/ml streptomycin sulfate. After 18 h, the medium was removed. Purified PCSK9 protein was labeled with Alexa Fluor 647 as described under "Experimental Procedures." Alexa Fluor 647-labeled PCSK9 (1, 5, or 20 μ g/ml) was added in 50 μ l of F-12K medium containing 10% lipoprotein-deficient serum to the cells. The plates were incubated at 37 °C for 4 h, and the cells were washed quickly with Tris-buffered saline before imaging. To label cellular nuclei, Hoechst 33342 at a final concentration of 0.1 μ g/ml was added to each well. The plates were run on an Opera imager

Secreted PCSK9 Regulates LDL Uptake

(Evotec Technologies GmbH, Hamburg, Germany) with a $\times 40$ water immersion objective. Images were captured using excitation wavelengths of 405 nm for fluorescent nuclei and 635 nm for Alexa Fluor 647-labeled PCSK9. For each well, 11 individual fields containing >500 cells were captured for two emission wavelengths. The data were analyzed using a customized algorithm written using the Acapella language (Evotec Technologies GmbH). The algorithm identified and marked the nuclear and cytoplasmic areas of individual cells, followed by measurement of the total cytoplasmic intensity of the cell. The intensity was expressed in arbitrary fluorescent units.

RESULTS

Expression and Purification of Gain- and Loss-of-function Mutant PCSK9 Proteins—Several mutations within PCSK9 that are associated with low or high levels of circulating LDL-C in humans have been described, and experiments in animals and cell culture indicate that PCSK9 action leads to degradation of the LDLR protein (14, 15, 17, 24). Notably, recent studies using gel-based methods have shown that PCSK9 binds specifically to LDLR *in vitro* and that the gain-of-function mutant D374Y has greater affinity for LDLR (6). We have expanded this work to understand and compare the effects of wild-type PCSK9, gain-of-function mutants S127R and D374Y, and loss-of-function mutant R46L on cellular LDL uptake, a measure of LDLR function. Several stable HEK293 cell lines expressing wild-type PCSK9 or loss-of-function (R46L) or gain-of-function (S127R and D374Y) mutations were generated. In addition, a control HEK293 cell line stably expressing vector alone (pcDNA) was also created. The PCSK9 proteins contained C-terminal V5 and His epitope tags, which enabled their detection and subsequent purification.

Secreted PCSK9 proteins were purified from the media of the stable HEK293 cell lines by affinity chromatography (TALON), followed by size exclusion and ion exchange (Mono Q) chromatography. Following purification, SDS-PAGE and Coomassie Blue staining showed that all PCSK9 proteins were highly pure ($>90\%$) (Fig. 1). Consistent with previously published data (6) the purified proteins consisted of the mature PCSK9 fragment containing the catalytic and C-terminal domains (~ 63 kDa) and the prodomain (~ 17 kDa). The fact that the two domains co-purified indicates that the affinity between these domains is very strong even after secretion. Notably, there was no evidence of further processing of the PCSK9 prodomain, which is typically required for activation of proprotein convertase protease activity (25, 26). Preparations of this highly pure PCSK9 protein were used in further biochemical analysis of PCSK9 function.

Exogenously Added PCSK9 Lowers Cellular LDL Uptake in Different Cell Lines—Recent work has shown that the transfer of medium from PCSK9-expressing cells to fresh cells results in down-regulation of both the number of LDLRs and, as a direct consequence, cellular LDL uptake (6, 19). In this study, we present a detailed analysis of the effects of purified secreted wild-type PCSK9 on LDL uptake in different cell lines. We examined the ability of wild-type PCSK9 to reduce LDL uptake in an HEK293 cell line stably expressing an empty pcDNA3.1 vector, a human hepatocyte cell line (HepG2), and a CHO cell line.

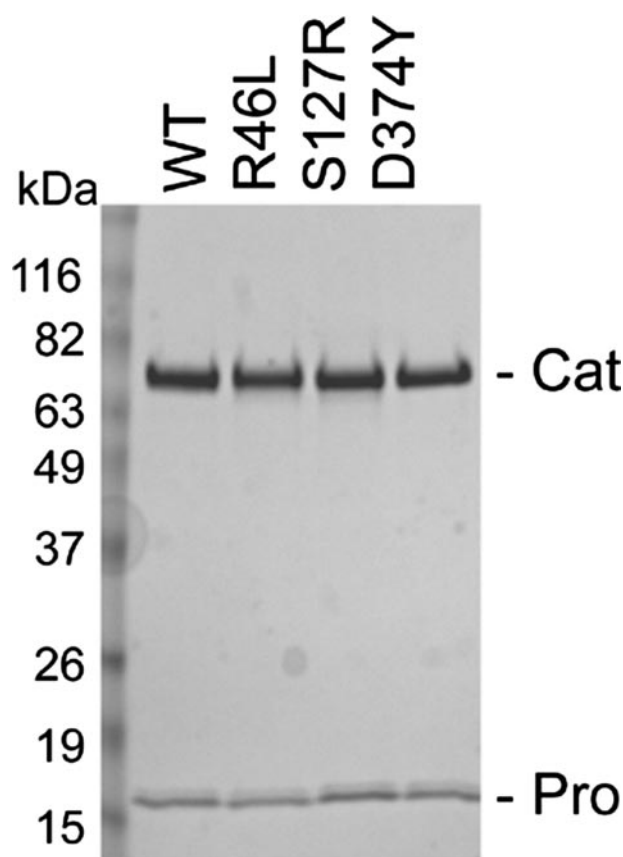


FIGURE 1. Purification of PCSK9 proteins secreted from HEK293 cell lines. Shown is a Coomassie Blue-stained gel of purified PCSK9 proteins. Stable HEK293 cell lines were maintained in $1\times$ DMEM containing 1 mg/ml G418 supplemented with 10% FBS. Following several days of growth, the medium was collected, and PCSK9 protein was purified through several chromatographic steps (TALON, size exclusion, and RESOURCE Q) as described under "Experimental Procedures". The results shown are from 1 μ g of recombinant PCSK9 protein loaded per well. *Cat* and *Pro* indicate the mature fragments of PCSK9 including the catalytic and cysteine-rich C-terminal domains and the prodomain of PCSK9, respectively. *WT*, wild-type PCSK9.

Analysis of basal LDL uptake by these cell lines demonstrated that all three cell lines internalize LDL to comparable levels, with HEK293 cells showing a slightly reduced level of LDL uptake compared with HepG2 and CHO cells (Fig. 2A). As shown in Fig. 2B, the addition of purified PCSK9 to the media of HEK293-pcDNA3.1, HepG2, and CHO cell lines reduced the amount of LDL uptake in a dose-dependent manner. The potency (EC_{50}) of PCSK9 in lowering LDL uptake was ~ 2 -fold weaker in CHO cells ($EC_{50} = 129 \pm 19$ nM; 9.7 μ g/ml) and similar in HepG2 cells ($EC_{50} = 64 \pm 16$ nM; 4.8 μ g/ml) compared with HEK293 cells ($EC_{50} = 61 \pm 21$ nM; 4.6 μ g/ml) (Fig. 2B).

LDL Uptake Lowering Potencies of Wild-type PCSK9 and Mutants R46L, S127R, and D374Y Correlate with LDL-C Levels in Humans Carrying Those Mutations—To determine whether the relative potencies of PCSK9 mutations in LDL uptake may help explain their effects on LDL concentrations in humans carrying such mutations, we compared the potency of various PCSK9 mutants with that of the wild-type form of the protein. As shown in Fig. 2C, LDL uptake was reduced when increasing amounts of PCSK9 protein were added to the media. The amount of LDL uptake was reduced by 50% at a concentration

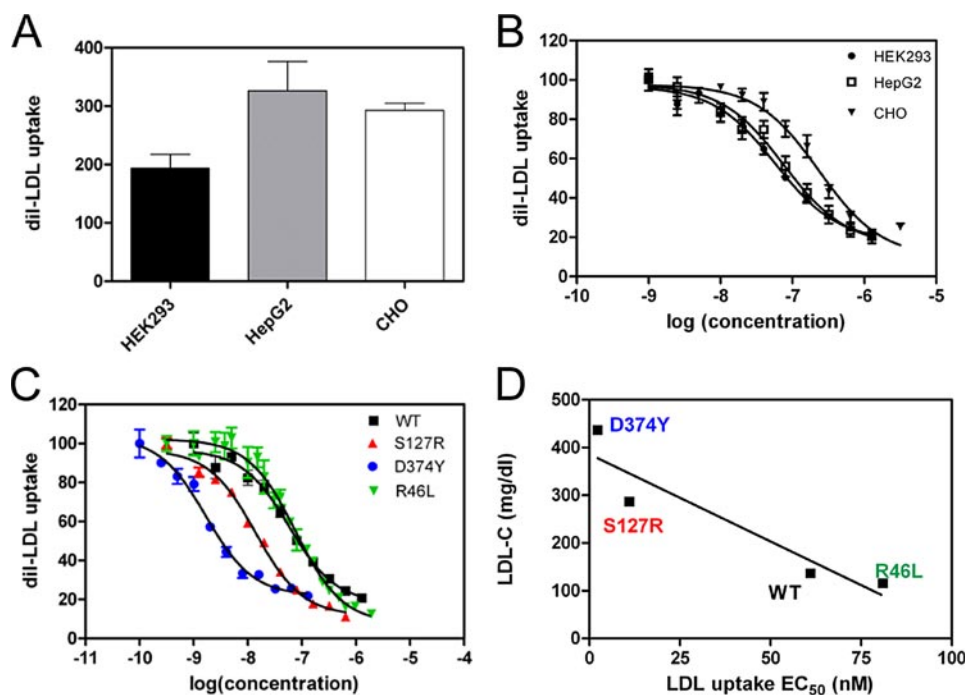


FIGURE 2. Reduction of LDL uptake by exogenously added PCSK9 protein. *A*, analysis of DiI-labeled LDL uptake by HEK293, HepG2, and CHO cell lines. Cells were grown and DiI-labeled LDL uptake was measured as described under "Experimental Procedures." *B*, purified PCSK9 protein inhibits LDL uptake in HEK293, HepG2, and CHO cell lines. Each cell line was grown in serum-free medium for 18 h before the addition of the indicated amounts of purified PCSK9 protein and DiI-labeled LDL. Following incubation for 6.5 h, cells were washed, and the amount of DiI-labeled LDL uptake was measured as described under "Experimental Procedures." The data shown are representative of at least three independent experiments and are fit to a sigmoidal dose-response curve by nonlinear regression. *C*, PCSK9 gain-of-function mutants D374Y and S127R decrease LDL uptake more efficiently than wild-type PCSK9 or loss-of-function mutant R46L. *D*, relationship between the apparent biochemical potency of various PCSK9 mutants (*horizontal axis*) versus the LDL-C levels in humans bearing those same mutations (*vertical axis*). Shown are the mean EC_{50} values determined in the cell-based assay of PCSK9 function and the mean LDL concentrations from human subjects found in published reports (7, 13, 44).

TABLE 1

LDL uptake results and relationship between EC_{50} values and LDL concentrations in humans

The potencies of wild-type (WT) and mutant PCSK9 proteins in inhibiting LDL uptake were determined with a pcDNA3.1 cell line as described under "Experimental Procedures."

Genotype	LDL uptake EC_{50} ^a	Gain/loss ^b	LDL-C ^{c,d}	No. individuals
	nM		mg/dl	
WT	61 ± 21		137 ± 37	9223
R46L	81 ± 6.7	Loss	116 ± 33	301
S127R	11 ± 4.6	Gain	287 ± 72	9
D374Y	2.3 ± 0.9	Gain	437 ± 158	13

^a Concentration of PCSK9 protein at which 50% of LDL uptake was inhibited (means ± S.D.).

^b Indicates whether the PCSK9 mutation results in hypercholesterolemia (gain) or hypocholesterolemia (loss).

^c Denotes average LDL-C concentration present in plasma from individuals bearing the indicated PCSK9 genotype.

^d LDL-C concentrations for the following PCSK9 genotypes obtained as indicated: wild-type PCSK9 (13), R46L (13), S127R (7), and D374Y (44).

of 61 ± 21 nM ($4.6 \mu\text{g/ml}$) for wild-type PCSK9 protein (Table 1). By comparison, both the S127R and D374Y gain-of-function proteins were significantly more effective in reducing the amount of LDL uptake by cells. S127R was ~5-fold more effective in reducing LDL uptake ($EC_{50} = 11 \pm 4.6$ nM; $0.86 \mu\text{g/ml}$), and D374Y was ~25-fold more effective ($EC_{50} = 2.3 \pm 0.9$ nM; $0.18 \mu\text{g/ml}$) (Table 1). The ability of the R46L loss-of-function mutant to reduce LDL uptake was similarly tested to determine whether it is less effective than wild-type PCSK9 protein. The

R46L protein was slightly less effective than the wild-type protein in reducing LDL uptake ($EC_{50} = 81 \pm 6.7$ nM; $6.3 \mu\text{g/ml}$). Of note, the potencies (EC_{50}) of the different PCSK9 proteins correlated linearly with the LDL-C concentrations of humans carrying such mutations (Fig. 2D). A similar trend in potencies was observed when the D374Y gain-of-function mutant was added to the HepG2 and CHO cell lines, with the following results: HepG2 cells, $EC_{50} = 3.5 \pm 1.6$ nM ($0.27 \mu\text{g/ml}$); and CHO cells, $EC_{50} = 6.9 \pm 2.3$ nM ($0.53 \mu\text{g/ml}$). Together, these data demonstrate that measuring the ability of purified PCSK9 proteins to reduce cellular LDL uptake provides a readout that correlates with the ability of PCSK9 to regulate LDLR function *in vivo*.

PCSK9 Directly Binds LDLR in a pH-dependent Manner—The experiments described above demonstrate that secreted PCSK9 reduces cellular LDL uptake in different cell lines. A previous study using gel blotting techniques has shown that PCSK9 binds LDLR specifically and that the D374Y gain-of-function mutant has greater affinity for

LDLR than does wild-type PCSK9 (6). Here, we use the methods of surface plasmon resonance (Biacore technology) and TR-FRET to measure and compare thermodynamic and kinetic parameters of LDLR binding by PCSK9, gain-of-function mutants S127R and D374Y, and loss-of-function mutant R46L. First, Biacore technology was used to measure the binding affinities of wild-type PCSK9 and mutants for the immobilized LDLR ectodomain at pH 7.4. A strong interaction between LDLR and PCSK9, but not a control protein, was detected (Fig. 3A). Comparison of the thermodynamic dissociation constants (K_D) at pH 7.4 showed that the affinity of the gain-of-function mutant D374Y for the receptor was 6–7 times higher than that of the wild-type protein (Fig. 3, A and B; and Table 2), consistent with the trend obtained by reported gel blotting studies (6). In contrast, at pH 7.4, the other gain-of-function mutant, S127R, bound LDLR similarly compared with wild-type PCSK9, whereas the loss-of-function mutant R46L had a 2-fold weaker affinity for LDLR compared with wild-type PCSK9 (Table 2).

LDL binds to LDLR at neutral pH on the cell surface, but the complex dissociates at the low pH of the endosomes (pH < 6) (27–29). Therefore, we thought to determine whether the PCSK9-LDLR interaction would also be affected by exposure to acidic pH. Biacore experiments were repeated at pH 5.3, and the K_D values for all mutants were obtained. Surprisingly, the affinity of all PCSK9 proteins for LDLR at pH 5.3 was at least 150-fold higher than that at pH 7.4, resulting in K_D values in the

Secreted PCSK9 Regulates LDL Uptake

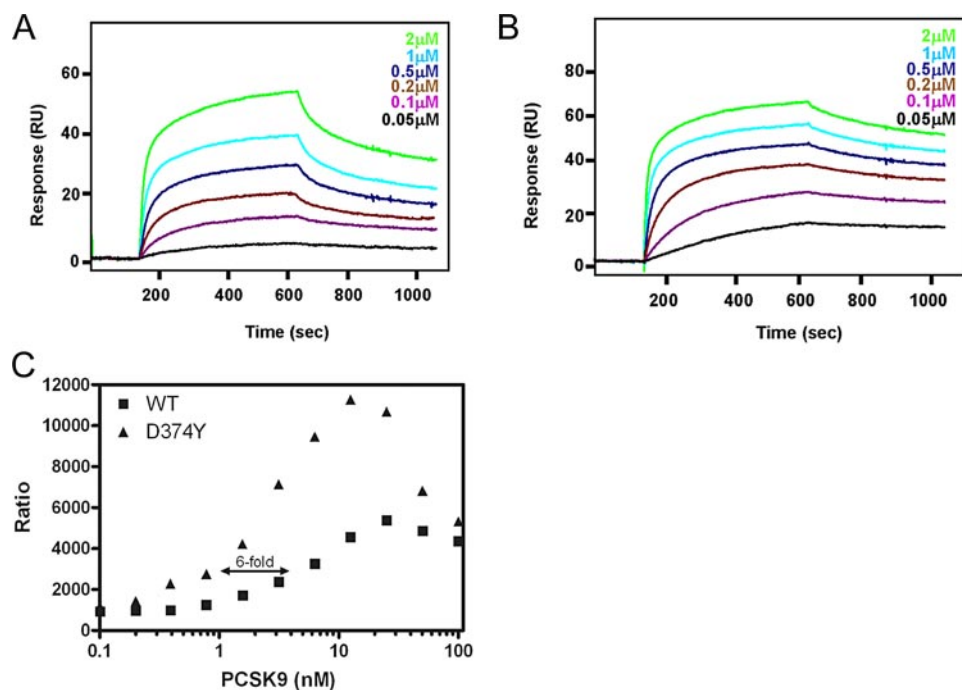


FIGURE 3. PCSK9 binds specifically to LDLR. *A*, solution-phase PCSK9-LDLR binding measured by surface plasmon resonance (Biacore). A representative Biacore sensorgram shows the response over time (resonance units (RU)) during the binding at pH 7.4 of purified recombinant wild-type PCSK9 to immobilized recombinant LDLR ectodomain. *B*, titration curve for binding of the purified PCSK9 mutant D374Y to immobilized recombinant LDLR ectodomain at pH 7.4. A slower dissociation of the complex was observed for the gain-of-function mutant D374Y compared with wild-type PCSK9. *C*, TR-FRET indicates that D374Y is ~6-fold more potent than the wild-type protein in binding to europium-labeled LDLR. A preformed complex of Alexa Fluor 647-labeled anti-V5 antibody (40 nm) and Eu³⁺-labeled recombinant LDLR ectodomain (15 nm) was combined with increasing amounts of purified wild-type PCSK9 protein or the D374Y mutant at pH 7.4. The specific fluorescence transfer (*Ratio*) was detected between a europium-labeled LDLR ectodomain and PCSK9 bound to Alexa Fluor 647-labeled anti-V5 antibody.

TABLE 2
LDLR binding affinities for wild-type PCSK9 and mutants at pH 7.4 and 5.3

The binding affinities of wild-type and mutant PCSK9 proteins for LDLR were determined at pH 7.4 and 5.3 as described under "Experimental Procedures."

Genotype	k_{on}	\times^{WT^a} k_{on}	k_{off}	\times^{WT} k_{off}	K_D	\times^{WT} K_D
	$M^{-1} s^{-1}$		s^{-1}		<i>nM</i>	
pH 7.4						
WT	1.86×10^3	1.0	1.17×10^{-3}	1.0	628	1.0
R46L	5.26×10^3	2.8	6.31×10^{-3}	5.3	1200	1.9
S127R	1.19×10^4	6.3	7.72×10^{-3}	6.5	648	1.03
D374Y	4.57×10^3	2.4	4.62×10^{-4}	0.4	101	0.16
pH 5.3						
WT	4.73×10^5	1.0	1.97×10^{-3}	1.0	4.19	1.0
R46L	1.38×10^5	0.3	8.72×10^{-3}	4.4	6.33	1.5
S127R	8.13×10^5	1.7	1.42×10^{-3}	0.7	1.76	0.4
D374Y	6.74×10^5	1.4	3.64×10^{-4}	0.2	0.54	0.1

^a-Fold change from wild-type PCSK9 at the indicated pH.

low nanomolar range (Table 2). Finally, similar to what was observed at neutral pH, at pH 5.3, the R46L mutant had a modestly lower affinity (1.5–2-fold weaker). In contrast, the S127R mutant showed a modestly higher affinity (2-fold stronger) compared with wild-type PCSK9 at pH 5.3 (Table 2). To further validate the results obtained by Biacore, TR-FRET-based experiments (22, 23) were used to measure the interaction between PCSK9 and LDLR. Specific fluorescence transfer was detected between a Eu³⁺-labeled LDLR ectodomain and PCSK9 bound to Alexa Fluor 647-labeled anti-V5 antibody at pH 6.8. As shown in Fig. 3C, the concentration of D374Y pro-

tein required for significant detection of PCSK9-LDLR-dependent fluorescence was ~36-fold lower than that of wild-type PCSK9, indicating a much higher affinity between D374Y and LDLR. Together, these experiments independently show that the D374Y mutant bound LDLR with greater affinity than did wild-type PCSK9 (Fig. 3C).

PCSK9 Is Internalized by Cultured Cells and the D374Y Mutant Is Internalized More Efficiently Compared with Wild-type PCSK9 and the S127R and R46L Mutants—Immunoblot experiments have previously shown that wild-type PCSK9 is internalized when added to fresh cells and that the gain-of-function mutant D374Y is internalized more efficiently (6). To expand on this work and to compare other PCSK9 mutants, confocal microscopy was used to measure the relative uptake efficiencies of PCSK9 and gain-of-function mutants D374Y and S127R and loss-of-function mutant R46L. To measure PCSK9 internalization, we directly labeled PCSK9 with Alexa Fluor

647. Labeling PCSK9 with the dye did not significantly affect its ability to reduce LDL uptake because the relative potency of labeled PCSK9 was reduced modestly (3-fold) compared with the unlabeled protein (data not shown). The uptake of DiI-labeled LDL by CHO cells was significantly reduced in the presence of 20 μg/ml Alexa Fluor 647-labeled wild-type or D374Y protein (Fig. 4A, left panels), confirming the activity of Alexa Fluor 647-labeled PCSK9 in lowering LDL uptake. To measure PCSK9 uptake, CHO cells were incubated with Alexa Fluor 647-labeled PCSK9, and the uptake of PCSK9 was quantified by confocal microscopy (Fig. 4A, right panels). The uptake of Alexa Fluor 647-labeled wild-type PCSK9 protein by CHO cells was detectable within 30 min after addition to cells (data not shown). In addition to wild-type PCSK9 protein, Alexa Fluor 647-labeled gain-of-function (S127R and D374Y) and loss-of-function (R46L) proteins were also taken up by cells (Fig. 4). Based on experiments in which a subsaturating concentration of Alexa Fluor 647-labeled PCSK9 was added to cells (1 μg/ml) and the relative intensities of internalized Alexa Fluor 647-labeled PCSK9 protein within cells, the D374Y protein was internalized ~3-fold more efficiently than the wild-type protein, whereas both the S127R and R46L mutants were taken up by cells to a similar extent as the wild-type protein (Fig. 4B). A similar pattern of PCSK9 uptake was also observed using HEK293 cells (data not shown), indicating that the D374Y protein is internalized more efficiently by cells.

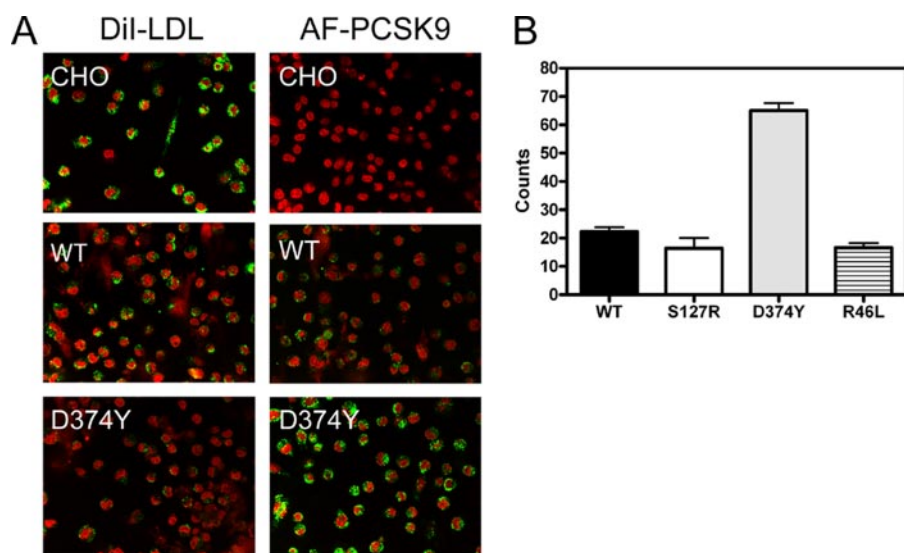


FIGURE 4. Cellular internalization of wild-type and mutant PCSK9. *A*, imaging of DiI-labeled LDL and wild-type PCSK9 and mutant D374Y protein uptake into CHO cells. *Left panels*, CHO cells were incubated with 10 $\mu\text{g/ml}$ DiI-labeled LDL (*DiI-LDL*) in the presence or absence of 20 $\mu\text{g/ml}$ (250 nM) Alexa Fluor 647-labeled wild-type (*WT*) PCSK9 or mutant D374Y protein for 4 h before images were obtained by confocal microscopy. *Right panels*, CHO cells were incubated with 5 $\mu\text{g/ml}$ (62.5 nM) Alexa Fluor 647-labeled PCSK9 (*AF-PCSK9*) proteins. Images shown are at $\times 40$ scale. *B*, quantification of wild-type and mutant PCSK9 uptake into CHO cells. The amount of Alexa Fluor 647-labeled PCSK9 uptake into cells was quantified as described under "Experimental Procedures." The results shown are with 1 $\mu\text{g/ml}$ (12.5 nM) labeled PCSK9 added and are representative of at least three independent experiments.

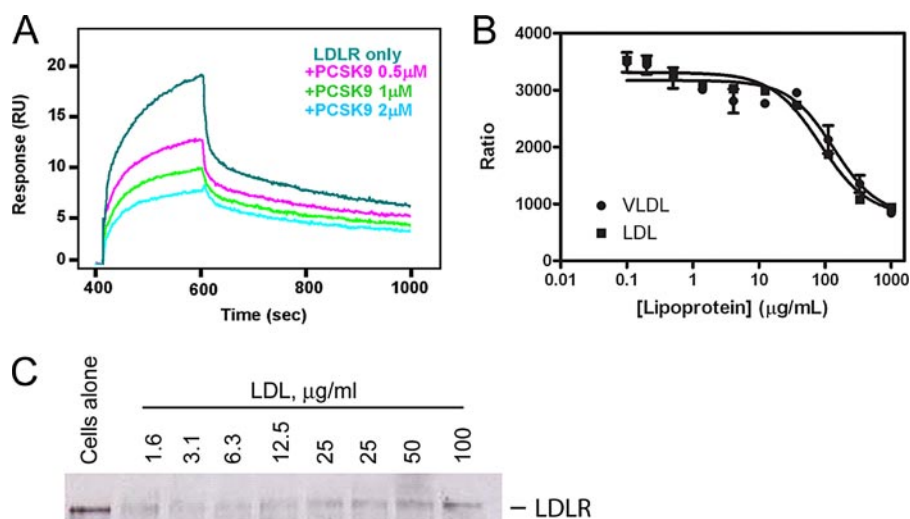


FIGURE 5. LDL competes with PCSK9 for LDLR binding and inhibits PCSK9 function. *A*, Biacore sensorgrams show that the binding of LDLR to immobilized LDL particles is reduced when LDLR (130 nM) is preincubated with increasing concentrations of wild-type PCSK9 protein, indicating a competition between PCSK9 and LDL for LDLR binding. *B*, both LDL and VLDL disrupt the complex between europium-labeled soluble LDLR and wild-type PCSK9. In this titration, increasing amounts of either VLDL or LDL were titrated into reactions containing a preformed complex of Alexa Fluor 647-labeled anti-V5 antibody (40 nM), wild-type PCSK9 (80 nM), and Eu^{3+} -labeled recombinant LDLR (12 nM) at pH 7.4. Data are the means \pm S.D. of triplicates. Curve fits are three-parameter fits with the bottom set as the no-PCSK9 background. *C*, the results from LDLR Western blot analysis show that the effects of exogenous PCSK9 on LDLR degradation are inhibited by LDL in a dose-dependent manner. The pcDNA3.1 cell line was treated with or without 25 $\mu\text{g/ml}$ PCSK9 and increasing amounts of LDL. The data shown are representative of three independent experiments. In each lane, the sample loaded onto the gel was normalized for total cellular protein. *RU*, resonance units.

LDL and VLDL Decrease LDLR Binding Affinity for PCSK9—Both LDL and VLDL particles bind LDLR and are released within endosomes for catabolism. In light of the observed interaction between LDLR and PCSK9, we investigated the effects of LDL and VLDL on the affinity of PCSK9 for LDLR using biosensor- and TR-FRET-based experiments. For the

first set of experiments, PCSK9 was immobilized on a sensor chip, and the LDLR ectodomain was injected at a single concentration. The sensogram obtained was consistent with the interaction previously observed between immobilized LDLR and injected PCSK9 (data not shown). We then tested whether LDL could bind directly to immobilized PCSK9; however, no interaction was detected (maximum concentration of injected LDL was 65 $\mu\text{g/ml}$ (130 nM)) (data not shown). We then immobilized LDL on the sensor chip and observed specific binding to LDLR (Fig. 5*A*), but not to PCSK9 (up to 1 μM added). The K_D of LDL for LDLR in this experiment was 11 nM (data not shown), a value consistent with published reports (40–42). Finally, a direct competition experiment between LDL and PCSK9 for LDLR binding was performed (Fig. 5*A*). In this experiment, LDLR (130 nM) was first incubated at room temperature with increasing concentrations of wild-type PCSK9 protein, and samples were then injected over immobilized LDL particles. A comparison of the sensorgrams showed a diminishing response with increasing PCSK9 concentrations (Fig. 5*A*), indicating that PCSK9 decreases the affinity of LDLR for LDL either by causing a conformational change on the receptor (*i.e.* allosteric effect) or by reducing the accessibility of the LDL-binding site on LDLR.

To confirm the effects of LDL on PCSK9-LDLR binding, we titrated LDL and VLDL particles to a preformed fluorescently labeled LDLR-PCSK9 complex at pH 7.4 (see "Experimental Procedures"). As the amount of either LDL or VLDL was increased in the reaction, the TR-FRET ratio between the preformed LDLR-PCSK9 complexes

decreased (Fig. 5*B*), indicating that these lipoprotein particles cause dissociation of the complex. LDL was ~ 2 -fold more efficient at disrupting the LDLR-PCSK9 complex ($\text{IC}_{50} = 84 \pm 15 \mu\text{g/ml}$) compared with VLDL ($\text{IC}_{50} = 134 \pm 35 \mu\text{g/ml}$). Therefore, LDL and VLDL not only bind tightly to LDLR, but also affect PCSK9 binding to LDLR.

Secreted PCSK9 Regulates LDL Uptake

LDL Inhibits PCSK9-dependent Effects on Cellular LDLR Degradation—To examine the effects of LDL on PCSK9 function in cell culture, PCSK9 was added to HEK293 cells for 6 h in either the absence or presence of increasing amounts of LDL (1.6–100 $\mu\text{g/ml}$), and LDLR was detected in whole cell lysate by Western blotting (Fig. 5C). In the absence of LDL, PCSK9 degraded whole cell LDLR to levels below detection; however, at LDL concentrations of 25 $\mu\text{g/ml}$ and above, the effects of PCSK9 on LDLR degradation were partially blocked (Fig. 5C). Notably, the addition of LDL alone did not affect the amount of whole cell LDLR protein levels (data not shown), indicating that the increase in LDLR observed in the presence of PCSK9 and LDL is likely due to LDL preventing PCSK9-dependent degradation of LDLR. Together, these results and the *in vitro* PCSK9-LDLR binding data suggest that LDL exerts an inhibitory effect on the PCSK9-dependent degradation of LDLR by modulating PCSK9-LDLR binding.

DISCUSSION

In this study, we have presented biochemical and cell-based data that deepen our understanding of the mechanism by which secreted PCSK9 promotes LDLR degradation. Recent work has shown that, when added to fresh cultured HepG2 cells, processed PCSK9 lowers cell-surface LDLR and whole cell LDLR (6). We have confirmed this result and expanded upon it by showing that highly purified and processed PCSK9 lowers cellular LDL uptake in three different cell lines (HEK293, HepG2, and CHO). In our studies, all three cell lines had comparable basal LDL uptake levels that was lowered in a dose-dependent manner by exogenously added wild-type PCSK9, with the maximum potency achieved in HEK293 cells ($EC_{50} = 61 \text{ nM}$; 4.6 $\mu\text{g/ml}$), followed by HepG2 cells ($EC_{50} = 64 \text{ nM}$; 4.8 $\mu\text{g/ml}$) and CHO cells ($EC_{50} = 129 \text{ nM}$; 9.7 $\mu\text{g/ml}$) (Fig. 2B). The potency ($EC_{50} = 4.6 \mu\text{g/ml}$) of wild-type PCSK9 in lowering LDL uptake in HepG2 cells was ~ 3 -fold weaker than the potency for LDLR degradation recently reported by Horton and co-workers (6). This discrepancy is likely related to the differences in the lipoprotein content of the incubation media. In our LDL uptake assay system, PCSK9 was added in the presence of 10 $\mu\text{g/ml}$ DiI-labeled LDL to medium containing 10% lipoprotein-deficient serum, whereas the LDLR degradation experiments were carried out with medium lacking LDL and containing 5% lipoprotein-deficient serum. We consistently found that the EC_{50} for LDLR degradation by PCSK9 was shifted ~ 3 -fold toward weaker potencies in the presence of 10 $\mu\text{g/ml}$ LDL (data not shown).

Although several studies have reported that PCSK9 is functionally active in HEK293 and HepG2 cells (5, 6, 15, 19), one report indicates that CHO cells stably expressing PCSK9 do not have lower LDLR compared with mock cells, indicating that PCSK9 is not functional in CHO cells (15). In this study, we used a functional cell-based assay (Fig. 2) and confocal imaging microscopy (Fig. 4) to show that wild-type PCSK9 and the gain-of-function mutant D374Y are functionally active in lowering LDL uptake and degrading LDLR in CHO cells. Our results suggest that either the levels of PCSK9 expression were too low and/or the concentration of PCSK9 in the medium was subop-

timal in the reported CHO cell line to have an impact on LDLR protein levels.

Our studies focused on two gain-of-function mutants (S127R and D374Y) and one loss-of-function mutant (R46L) that commonly occur in the human population (7–9, 12, 13, 30) and that undergo processing and secretion (15, 30, 31). Highly purified processed forms of PCSK9 proteins lower cellular LDL uptake when added to HEK293 cells with relative potencies that linearly correlate with plasma LDL-C levels in humans (Fig. 2D and Table 1). The potencies of gain-of-function mutants D374Y ($2.3 \pm 0.9 \text{ nM}$; 0.18 $\mu\text{g/ml}$) and S127R ($11 \pm 4.6 \text{ nM}$; 0.86 $\mu\text{g/ml}$) were significantly greater than those of wild-type PCSK9 ($61 \pm 21 \text{ nM}$; 4.6 $\mu\text{g/ml}$) and the loss-of-function mutant R46L ($81 \pm 6.7 \text{ nM}$; 6.3 $\mu\text{g/ml}$). In this work, we observed that the S127R mutant was ~ 5 -fold more potent than wild-type PCSK9 in lowering LDL uptake in HEK293 cells; a similar trend was observed in HepG2 cells as well (data not shown). In comparison, it has been reported that adenoviral overexpression of wild-type PCSK9 and S127R in mice promotes similar levels of hepatic LDLR degradation (15). This apparent discrepancy may result from dramatic overexpression induced by the adenoviruses, which may result in circulating levels of PCSK9 that are severalfold above the EC_{50} values of both proteins for lowering LDLR.

The relative LDL uptake lowering potencies of D374Y, S127R, wild-type PCSK9, and R46L (D374Y > S127R > wild-type PCSK9 > R46L) linearly correlate with LDL-C levels reported in humans carrying those mutations (Table 1) and parallel their LDLR binding affinities at pH 5.3 (Table 2). In comparison, the relative efficiency of cell internalization by PCSK9 and its mutants (D374Y > S127R = wild-type PCSK9 = R46L) more closely parallels their LDLR binding affinities at pH 7.4. These comparisons suggest that, although PCSK9-LDLR binding at the neutral pH of plasma is the rate-limiting step for PCSK9 entry into cells, PCSK9-LDLR binding at the acidic pH of endosomes also significantly influences PCSK9 activity on cellular LDL uptake. It is also likely that factors other than LDLR binding affinity contribute to regulate the functional activity of PCSK9 and its missense mutants. For example, it has been reported that the S127R protein is not processed as efficiently as wild-type PCSK9 or other PCSK9 missense mutants (5, 15), resulting in comparably less processed S127R protein secreted from cells. Despite this reduction in secretion, the S127R allele results in hypercholesterolemia (7). In addition, one report has found that wild-type PCSK9 can be cleaved by furin, but that gain-of-function mutants R218S, F216L, and D374Y are less susceptible to processing by furin (31). Therefore, it is likely that, in addition to PCSK9-LDLR affinity, other factors influence the activity of wild-type PCSK9 and its missense mutants in lowering LDLR levels *in vivo*.

LDLR binds its ligands (LDL, VLDL, and C7, a monoclonal antibody that recognizes the LDLR ligand-binding domain) at the cell surface, followed by internalization of the complex through endocytosis in clathrin-coated pits (28, 32, 33). At the low pH of endosomes (pH < 6), LDLR undergoes a conformational change leading to dissociation of the LDLR-ligand complex, recycling of the receptor to the cell surface, and degradation of the ligand in lysosomes (28, 29). In agreement with

recent work (6, 34), we have shown that PCSK9 interacts directly with LDLR (Fig. 3) and is internalized by cells (Fig. 4). However, we have shown that PCSK9 behaves quite differently from the other well characterized LDLR ligands in that its affinity for the receptor is significantly enhanced (>150-fold) at pH 5.3 compared with neutral pH (Table 2). It has been shown that dissociation of LDLR from LDL is required for LDLR recycling (27, 35); similarly, lack of dissociation of the LDLR-PCSK9 complex in the endosomes may prevent LDLR recycling and lead to shuttling of the complex to lysosomes for eventual degradation. Furthermore, a similar mechanism for LDLR degradation has been demonstrated previously using an LDLR deletion mutant lacking the epidermal growth factor precursory homology domain. This mutant form of the receptor is displayed at the cell surface, binds VLDL (but not LDL), and is internalized into cells like the wild-type receptor; however, it cannot dissociate from VLDL in endosomes and, instead of being recycled, is directed to the lysosome for degradation (27, 35). Of note, degradation of LDLR upon overexpression of PCSK9 in cultured cells is blocked by the addition of NH_4Cl , indicating a role for a pH-sensitive compartment such as the lysosome in PCSK9-dependent LDLR degradation (5, 36). Although we cannot exclude that PCSK9 acts as a protease upon LDLR or another protein following internalization by cells and/or entry into an acidic microenvironment such as the endosomal or lysosomal compartment, we did not find any evidence of PCSK9-dependent LDLR degradation using purified proteins *in vitro* at both neutral and acidic pH (data not shown). Moreover, we and others (6) have not been successful in detecting PCSK9-specific cleavage of any peptide substrate, including those resembling the PCSK9 site of processing (FAQ ↓ SIP). Together, these data suggest a model in which PCSK9 functions as a shuttling protein by forcing the trafficking of LDLR to the lysosomes for degradation.

An important question is whether PCSK9 works during secretion out of the cell or during internalization (37). Overexpression of PCSK9 in the livers of mice lacking ARH (autosomal recessive hypercholesterolemia), a putative adaptor protein required for LDLR endocytosis (38, 39), results in a reduction of hepatic LDLR protein levels (15). This indicates that PCSK9 can reduce LDLR protein during transport to the cell surface or when LDLR is on the cell surface. However, in this system, PCSK9 was dramatically overexpressed, which could result in activation of an alternative pathway of PCSK9-dependent LDLR degradation. In comparison, our study and recent work (6, 19) indicate that processed secreted PCSK9 is functionally active because it can lower cell-surface LDLR protein and whole cell LDLR levels when added to fresh cultured cells. The ability of secreted PCSK9 to lower LDLR protein levels requires LDLR endocytosis, as there is no effect of PCSK9 addition to cultured cells lacking the ARH adaptor protein (6). Although our results show that secreted and internalized PCSK9 can lower LDLR function, further studies will be required to address the relative roles of PCSK9 in lowering LDLR before or after secretion *in vivo*.

Our data indicating that LDL and VLDL affect the LDLR binding affinity for PCSK9 and the partial inhibitory effect of LDL in cell culture suggest that the contribution of secreted

PCSK9 to LDLR lowering may be attenuated by the levels of plasma LDL. If the PCSK9 predominant site of action on LDLR is on the cell surface, then it is likely that circulating levels of LDL decrease the affinity of LDLR for PCSK9 by causing a conformational change in the receptor (*i.e.* allosteric effect) or by reducing the accessibility of PCSK9 to its binding site on LDLR. In fact, the binding affinity of wild-type PCSK9 for LDLR ($K_D = 628 \text{ nM}$) is significantly lower than that of LDL for LDLR (5–25 nM) (40–42), and the human plasma concentrations of PCSK9 (2–10 nM; $\sim 0.5 \mu\text{g/ml}$) (6) are much lower than that of LDL ($\sim 2.8 \mu\text{M apoB}$; $\sim 1500 \mu\text{g/ml}$) (43). However, complete inhibition of PCSK9 was not achieved even when excess LDL was used (data not shown), suggesting that additional factors such as the local concentrations of PCSK9 and LDL at the cell surface or an accessory cell-surface protein may play a role in modulating the PCSK9-LDLR interaction. The involvement of other factors such as a cell-surface accessory protein would also explain the discrepancy between the levels of plasma PCSK9 and the EC_{50} we obtained in our cell-based assay. In conclusion, we have shown that LDL partially inhibits the LDLR lowering activity of plasma PCSK9; moreover, we have shown that PCSK9 and LDLR form a highly stable complex at acidic pH, suggesting that PCSK9 prevents LDLR recycling and ultimately causes LDLR degradation by directing the receptor to the lysosomes.

Addendum—While this manuscript was under revision, two studies were published that show pH-dependent binding of PCSK9 to LDLR (45, 46).

REFERENCES

- Seidah, N. G., Benjannet, S., Wickham, L., Marcinkiewicz, J., Jasmin, S. B., Stifani, S., Basak, A., Prat, A., and Chretien, M. (2003) *Proc. Natl. Acad. Sci. U. S. A.* **100**, 928–933
- Steiner, D. F. (1998) *Curr. Opin. Chem. Biol.* **2**, 31–39
- Seidah, N. G., and Chretien, M. (1999) *Brain Res.* **848**, 45–62
- Naureckiene, S., Ma, L., Sreekumar, K., Purandare, U., Lo, C. D., Huang, Y., Chiang, L. W., Grenier, J. M., Ozenberger, B. A., and Jacobsen, J. S. (2003) *Arch. Biochem. Biophys.* **420**, 55–67
- Benjannet, S., Rhainds, D., Essalmani, R., Mayne, J., Wickham, L., Jin, W., Asselin, M.-C., Hamelin, J., Varret, M., Allard, D., Trillard, M., Abifadel, M., Tebon, A., Attie, A. D., Rader, D. J., Boileau, C., Brissette, L., Chretien, M., Prat, A., and Seidah, N. G. (2004) *J. Biol. Chem.* **279**, 48865–48875
- Lagace, T. A., Curtis, D. E., Garuti, R., McNutt, M. C., Park, S. W., Prather, H. B., Anderson, N. N., Ho, Y. K., Hammer, R. E., and Horton, J. D. (2006) *J. Clin. Invest.* **116**, 2995–3005
- Abifadel, M., Varret, M., Rabes, J.-P., Allard, D., Ouguerram, K., Devillers, M., Cruaud, C., Benjannet, S., Wickham, L., Erlich, D., Derre, A., Villegier, L., Farnier, M., Beucler, I., Bruckert, E., Chambaz, J., Chanu, B., Lecerf, J.-M., Luc, G., Moulin, P., Weissenbach, J., Prat, A., Krempf, M., Junien, C., Seidah, N. G., and Boileau, C. (2003) *Nat. Genet.* **34**, 154–156
- Leren, T. (2004) *Clin. Genet.* **65**, 419–422
- Timms, K. M., Wagner, S., Samuels, M., Forbey, K., Goldfine, H., Jammulapati, S., Skolnick, M., Hopkins, P., Hunt, S., and Shattuck, D. (2004) *Hum. Genet.* **114**, 349–353
- Cohen, J., Pertsemlidis, A., Kotowski, I. K., Graham, R., Garcia, C. K., and Hobbs, H. H. (2005) *Proc. Natl. Acad. Sci. U. S. A.* **37**, 161–165
- Berge, K. E., Ose, L., and Leren, T. P. (2006) *Arterioscler. Thromb. Vasc. Biol.* **26**, 1094–1100
- Kotowski, I., Pertsemlidis, A., Luke, A., Cooper, R. S., Vega, G. L., Cohen, J. C., and Hobbs, H. H. (2006) *Am. J. Hum. Genet.* **78**, 410–422
- Cohen, J. C., Boerwinkle, E., Mosley, T. H., Jr., and Hobbs, H. H. (2006) *N. Engl. J. Med.* **354**, 1264–1272

Secreted PCSK9 Regulates LDL Uptake

14. Maxwell, K. N., and Breslow, J. L. (2004) *Proc. Natl. Acad. Sci. U. S. A.* **101**, 7100–7105
15. Park, S. W., Moon, Y.-A., and Horton, J. D. (2004) *J. Biol. Chem.* **279**, 50630–50638
16. Lalanne, F., Lambert, G., Amar, M. J., Chetiveaux, M., Zair, Y., Jarnoux, A.-L., Ouguerram, K., Friburg, J., Seidah, N. G., Brewer, H. B., Jr., Krempf, M., and Costet, P. (2005) *J. Lipid Res.* **46**, 1312–1319
17. Rashid, S., Curtis, D. E., Garuti, R., Anderson, N. N., Bashmakov, Y., Ho, Y. K., Hammer, R. E., Moon, Y.-A., and Horton, J. D. (2005) *Proc. Natl. Acad. Sci. U. S. A.* **102**, 5374–5379
18. Graham, M. J., Lemonidis, K. M., Whipple, C. P., Subramaniam, A., Mohnia, B. P., Crooke, S. T., and Crooke, R. M. (2007) *J. Lipid Res.* **48**, 763–767
19. Cameron, J., Holla, O. L., Ranheim, T., Kulseth, M. A., Berge, K. E., and Leren, T. P. (2006) *Hum. Mol. Genet.* **15**, 1551–1558
20. Cooper, M. A. (2003) *Anal. Bioanal. Chem.* **377**, 834–842
21. Karlsson, R. (2004) *J. Mol. Recognit.* **17**, 151–161
22. Mathis, G. (1993) *Clin. Chem.* **39**, 1953–1959
23. Mathis, G. (1995) *Clin. Chem.* **41**, 1391–1397
24. Maxwell, K. N., Soccio, R. E., Duncan, E. M., Sehayek, E., and Breslow, J. L. (2003) *J. Lipid Res.* **44**, 2109–2119
25. Seidah, N., Khatib, A., and Prat, A. (2006) *Biol. Chem.* **387**, 871–877
26. Thomas, G. (2002) *Nat. Rev. Mol. Cell Biol.* **3**, 753–766
27. Davis, C. G., Goldstein, J. L., Sudhof, T. C., Anderson, R. G. W., Russell, D. W., and Brown, M. S. (1987) *Nature* **326**, 760–765
28. Brown, M. S., Anderson, R. G. W., and Goldstein, J. L. (1983) *Cell* **32**, 663–667
29. Rudenko, G., Henry, L., Henderson, K., Ichtchenko, K., Brown, M. S., Goldstein, J. L., and Deisenhofer, J. (2002) *Science* **298**, 2353–2358
30. Sun, X.-M., Eden, E. R., Tosi, I., Neuwirth, C. K., Wile, D., Naoumova, R. P., and Soutar, A. K. (2005) *Hum. Mol. Genet.* **14**, 1161–1169
31. Benjannet, S., Rhainds, D., Hamelin, J., Nassoury, N., and Seidah, N. G. (2006) *J. Biol. Chem.* **281**, 30561–30572
32. Innerarity, T. L., and Mahley, R. W. (1978) *Biochemistry* **17**, 1440–1447
33. Beisiegel, U., Schneider, W. J., Goldstein, J. L., Anderson, R. G., and Brown, M. S. (1981) *J. Biol. Chem.* **256**, 11923–11931
34. Grozdanov, P. N., Petkov, P. M., Karagoyozov, L. K., and Dabeva, M. D. (2006) *Biochem. Cell Biol.* **84**, 80–92
35. Miyake, Y., Tajima, S., Funahashi, T., and Yamamoto, A. (1989) *J. Biol. Chem.* **264**, 16584–16590
36. Maxwell, K. N., Fisher, E. A., and Breslow, J. L. (2005) *Proc. Natl. Acad. Sci. U. S. A.* **102**, 2069–2074
37. Horton, J. D., Cohen, J. C., and Hobbs, H. H. (2007) *Trends Biochem. Sci.* **32**, 71–77
38. He, G., Gupta, S., Yi, M., Michaely, P., Hobbs, H. H., and Cohen, J. C. (2002) *J. Biol. Chem.* **277**, 44044–44049
39. Garcia, C. K., Wilund, K., Arca, M., Zuliani, G., Fellin, R., Maioli, M., Calandra, S., Bertolini, S., Cossu, F., Grishin, N., Barnes, R., Cohen, J. C., and Hobbs, H. H. (2001) *Science* **292**, 1394–1398
40. Basu, S. K., Goldstein, J. L., and Brown, M. S. (1978) *J. Biol. Chem.* **253**, 3852–3856
41. Havekes, L., van Hinsbergh, V., Kempen, H. J., and Emeis, J. (1983) *Biochem. J.* **214**, 951–958
42. Nigon, F., Lesnik, P., Rouis, M., and Chapman, M. (1991) *J. Lipid Res.* **32**, 1741–1753
43. Goldstein, L. J., and Brown, S. M. (1977) *Annu. Rev. Biochem.* **46**, 897–930
44. Naoumova, R. P., Tosi, I., Patel, D., Neuwirth, C., Horswell, S. D., Marais, A. D., van Heyningen, C., and Soutar, A. K. (2005) *Arterioscler. Thromb. Vasc. Biol.* **25**, 2654–2660
45. Cunningham, D., Danley, D. E., Geoghegan, K. F., Griffor, M. C., Hawkins, J. L., Subashi, T. A., Varghese, A. H., Ammirati, M. J., Culp, J. S., Hoth, L. R., Mansour, M. N., McGrath, K. M., Seddon, A. P., Shenolikar, S., Stutzman-Engwall, K. J., Warren, L. C., Xia, D., and Qiu, X. (2007) *Nat. Struct. Mol. Biol.* **14**, 413–419
46. Zhang, D.-W., Lagace, T. A., Garuti, R., Zhao, Z., McDonald, M., Horton, J. D., Cohen, J. C., and Hobbs, H. H. (April 23, 2007) *J. Biol. Chem.* doi: 10.1074/jbc.M702027200

Effects of pH and Low Density Lipoprotein (LDL) on PCSK9-dependent LDL Receptor Regulation

Timothy S. Fisher, Paola Lo Surdo, Shilpa Pandit, Marco Mattu, Joseph C. Santoro, Doug Wisniewski, Richard T. Cummings, Alessandra Calzetta, Rose M. Cubbon, Paul A. Fischer, Anil Tarachandani, Raffaele De Francesco, Samuel D. Wright, Carl P. Sparrow, Andrea Carfi and Ayesha Sitlani

J. Biol. Chem. 2007, 282:20502-20512.

doi: 10.1074/jbc.M701634200 originally published online May 10, 2007

Access the most updated version of this article at doi: [10.1074/jbc.M701634200](https://doi.org/10.1074/jbc.M701634200)

Alerts:

- [When this article is cited](#)
- [When a correction for this article is posted](#)

[Click here](#) to choose from all of JBC's e-mail alerts

Supplemental material:

<http://www.jbc.org/content/suppl/2007/05/15/M701634200.DC1>

This article cites 46 references, 23 of which can be accessed free at <http://www.jbc.org/content/282/28/20502.full.html#ref-list-1>